

Article

Potentially Harmful Elements (As, Sb, Cd, Pb) in Soil Polluted by Historical Smelting Operation in the Upper Silesian Area (Southern Poland)

Weronika Nadłonek ¹, Jerzy Cabala ^{2,*}  and Krzysztof Szopa ² 

¹ Polish Geological Institute—National Research Institute, Królowej Jadwigi 1, 41-200 Sosnowiec, Poland; weronika.nadlonek@pgi.gov.pl

² Faculty of Natural Sciences, University of Silesia in Katowice, Będzińska 60, 41-200 Sosnowiec, Poland; krzysztof.szopa@us.edu.pl

* Correspondence: jerzy.cabala@us.edu.pl

Abstract: This study aimed at determining the concentration and possibility of migration of potentially harmful elements (PHEs) in soils and mining and metallurgical waste in the Silesian-Cracow region. Our research was carried out in selected locations of Ruda Śląska, Świętochłowice, Bytom, and in the Olkusz region (Bukowno) in southern Poland. The concentrations of metals (e.g., Ag, Ba, Ca, Cd, Cu, Fe, Mg, Mn, Pb, Sr, Zn), metalloids (As, Sb), and sulphur were determined in 33 soil samples (with a depth range of 0.0–0.3 m) and 12 slag samples. These studies show an increased concentration of metals, metalloids, and sulphur, exceeding the level of regional geochemical background. The research results indicate that the degree of the chemical transformation of soils in the analysed regions of Ruda Śląska, Bytom, and Bukowno is advanced. This highlights the high concentrations of most metals, i.e., arsenic, antimony, and sulphur, in the surface layer of soils (topsoil) due to historic Zn-Pb ore mining and Zn and Fe metallurgy. The presence of both primary and secondary metal sulphides, sulphates, carbonates, oxides/hydroxides, silicates, and aluminosilicates was found in the mineral composition of soils and slags.

Keywords: soil contamination; historical Zn-Pb smelting; arsenium; antimonium; cadmium; lead



Citation: Nadłonek, W.; Cabala, J.; Szopa, K. Potentially Harmful Elements (As, Sb, Cd, Pb) in Soil Polluted by Historical Smelting Operation in the Upper Silesian Area (Southern Poland). *Minerals* **2024**, *14*, 475. <https://doi.org/10.3390/min14050475>

Academic Editors: Yinxian Song, Yubo Wen and Ming Ma

Received: 12 April 2024

Revised: 25 April 2024

Accepted: 26 April 2024

Published: 29 April 2024



Copyright: © 2024 by the authors. Licensee MDPI, Basel, Switzerland. This article is an open access article distributed under the terms and conditions of the Creative Commons Attribution (CC BY) license (<https://creativecommons.org/licenses/by/4.0/>).

1. Introduction

In southern Poland, the mining and processing of Pb-Ag ores began in the 12th century on supergene ore deposits found in Triassic dolomites [1]. In the following centuries, Pb and Ag ore mining in the Silesian-Cracow region developed in the vicinity of mining towns founded under the Magdeburg Law, such as Bytom, Tarnowskie Góry, Olkusz, and Jaworzno. In the second half of the 18th century, coal mining and Fe smelting developed intensively in the area. Then, at the beginning of the 19th century, large-scale zinc production began in Upper Silesia using horizontal retorts designed (the so-called Silesian method) by J. Ch. Ruberg in 1798. Numerous mines, ore beneficiation plants, and Zn smelters were established in the 19th century and early 20th century. At the beginning of the 20th century, higher world-class Zn production was being exploited only in the USA and Belgium. In the area of Bytom, Ruda Śląska, Piekary Śląskie, Chorzów, and Katowice, metallurgical production was carried out by German, American, and French companies. Significant amounts of metallurgical waste with varied composition have been deposited around the historic Zn-Pb smelters [2,3]. The differentiation of the chemistry of these historical slags may be related to the technology of smelting, the mineral composition of the tailings, and the conditions of the weathering.

From the beginning of the 19th century, industrial production of Zn, Cd, Al, Cu, and other metals began in Europe. Among the components of the metallurgical charge, zinc carbonates, silicates, and lead carbonates dominated, while metal sulphides were less

prevalent than Zn and Pb carbonates. Until the beginning of the 20th century, oxidised ores were the primary source of zinc globally, and in the 20th century, their resources gradually ran out [4,5]. After World War I, the increase in zinc production was associated with developing zinc sulphide flotation methods and managing Zn-Pb sulphide ore resources. Consequently, the mineral composition of the metallurgical charge, dominated by Zn and Pb sulphides, changed. With the high profitability of zinc production, at the end of the 1920s, 33 zinc smelters were operating in the region of Upper Silesia and Dąbrowa Becken (Zagłębie Dąbrowskie). New applications of metals influenced their high prices and rapidly growing demand, which stimulated the development of mining and metallurgy of non-ferrous metals and their alloys. In the case of Zn, Cu, and Pb smelters, accompanying metals, such as Ag, Cd, and Bi, were recovered as a by-product. Non-ferrous metals were used in the production of alloys. A consequence of the production of metals was tailings waste deposited in the vicinity of steel mills. They were often slags, sludges, and waste from the metal refining processes. This waste can be enriched with metals found in alloys, synthetic phases, and relics of the primary minerals. They can also degrade the environment [1,6]. Identifying the type of mineral phases (see Supplementary Material) in the waste helps determine what metal smelting technologies were used in the past and whether the minerals are susceptible to chemical transformations such as weathering. In many regions in Europe, the environment has been polluted with heavy metals from Zn-Pb ore enrichment and Zn and Pb metallurgy. In the 19th and 20th centuries, in the vicinity of steel mills and mines, waste was deposited that has survived to the present day. Slags from Zn-Pb smelters are described from Spain [7], Belgium [8], Germany [9,10], and Poland [1,11,12].

Inefficient enrichment and metal production technologies and waste disposal methods contributed to high soil, water, and atmospheric pollution in Zn, Pb, Cd, Cu, Al, Ni, and other element production [13,14]. Minerals, both ferrous and non-ferrous metals deposited into the soil by mining, can be a source of bioavailable, toxic metal ions for at least 200 years [15,16]. Therefore, the effects of the historical production of non-ferrous metals are still felt today [17]. The areas affected by Zn and Pb mining and metallurgy are polluted by metals such as Zn, Pb, Sb, As, Mn, Tl, and Cd [18,19]. Research on slags from historical Pb-Ag metallurgy [1,20], Zn-Pb [1,21], and Ni-Co [22,23] provides information on synthetic phases containing Zn, Pb, Cd, Cu, and Ni, as well as As and Sb. The geochemical activity of metals and metalloids and their ability to form different phases varies with the environment. It is different from primary sulphide (reduced) ores and oxidised ores. Elements in alloys or synthetic phases of products of metallurgical processes have other geochemical characteristics.

The aims of this research are to determine the behaviour of the most PHEs (e.g., As, Sb, Cd, and Pb) in the smelting stage and weathering process. Indicating what phases they are and whether there is a risk of them being starting metals and metalloids from the slag silicate, carbonate, or oxide matrix is also important. Identifying synthetic and secondary phases rich in metalloids (As, Sb) and metals (e.g., Cd, Pb, Ag, Fe, Mn) may help us to understand the conditions for forming metal-bearing phases building slags, as determining the type of charge used in the metallurgical process. Identifying indicator metals in slags and contaminated soils can assess the kind of historical production carried out in smelters. Due to the high contents of As, Sb, and Ag in some ores from the Silesian-Cracow region [24], other geochemical pathways for these elements are interesting.

2. Historical Background

In Europe, zinc production began in the 18th century when Andreas Marggraf isolated (1746) pure zinc by reducing oxidised zinc ores with charcoal. William Champion developed a vertical zinc smelting retort and started the first ironworks in England (Bristol) in 1743. At the end of the 18th century, zinc was produced in England, Belgium, and Upper Silesia (Poland). The development of the production of this metal was related to the access to Zn-Pb deposits and hard coal necessary for the metallurgical process. Investments in zinc smelting

and iron alloys with Zn, Cu, Ni, V, Ti, Cr, and Pb were very profitable. In the areas where metal and coal deposits are present, a consolidation of steel mills, steel plants, galvanising plants, and metallurgical plants took place. In 1810, the Société de la Vieille Montagne was established in Belgium; the smelters had the most significant zinc production potential in the 19th century. Together with Belgian and American centres, Upper Silesia became one of the world's largest producers of Zn and Cd [25] (Popiołek 1965). Zinc smelters in Belgium (Liege, Aachen), Germany (Ruhr Area), and the USA (Illinois) operated on similar technological advances.

Within the limits of the cities of Upper Silesia (Katowice, Bytom, Ruda Śląska, Świętochłowice) and Dąbrowa-Becken (Dąbrowa Górnicza, Sosnowiec, Będzin), several Zn and Pb smelters, accompanied by installations for the production of Cd and Ag, were launched in the 19th century. At the beginning of the 19th century, investments in the mining of Zn-Pb ores and the production of Zn were carried out, among others, by Karol Godula (19 calamine ore mines, 3 Zn smelters), owned by Prussian private companies, e.g., Bergwerksgesellschaft Georg von Giesches Erben (2 Zn-Pb mines, 5 Zn and Pb, and one Pb smelter), Hohenlohe Werke AG (3 Zn smelters), owned by the Prussian Government (3 Zn smelters and one Pb), owned by the Polish Government and the Franco-Russian Society (3 Zn smelters and 6 calamine ore mines), and controlled by the Austro-Hungarian Government (2 Zn smelters, 4 calamine mines) [25–27]. The owners of Zn and Pb smelters also had coal mines.

The improvement in the metallurgical methods of Zn production significantly increased the profitability of production. In 1798, in Silesia (now Southern Poland), J. Ch. Ruberg implemented a more economical way of continuous Zn production using horizontal retorts [28]. Further technological progress in Zn production dates back to 1838 in Belgium. This process improved the thermal efficiency of the Zn smelting process and became the standard production method in the mid-19th century. The Silesia-Kracow region of Zn-Pb deposits covered a part of Upper Silesia, in Dąbrowa-Becken and Małopolska. These areas, until 1922, were within the borders of the kingdoms of Prussia, Austria-Hungary, and Russia. In the 19th century, this area was the location of a significant part of the world's Zn, Cd, and Pb production. At the beginning of the 20th century, higher Zn production was obtained only in the USA and Belgium. In addition, in Upper Silesia, Zn was used to produce brass alloys, red brass, and high-Ni brass, so-called argentan. Significant amounts of post-metallurgical waste with varied phases and compositions have been deposited around the historic Zn-Pb smelters [2,3].

The Zn and Pb smelters operating in Bytom and Ruda Śląska in the 19th and 20th centuries mainly used oxidised Zn-Pb ores. Among the components of the metallurgical charge, Zn carbonates and silicates, as well as Pb carbonates, dominated, while the proportion of Zn-Pb sulphides was lower. Until the beginning of the 20th century, oxidised ores were the primary source of Zn globally, and in the 20th century, their resources gradually ran out [4,5]. The increase in Zn production was related to the development of Zn sulphide flotation methods and managing Zn-Pb sulphide ores. In the 19th and 20th centuries, technologies for producing Zn and Pb and recovering the accompanying metals (i.e., Ag, Cd) were improved. The metallurgical charge was enriched oxidised ores, and at the end of the 19th century, sulphide concentrates and older, metal-rich waste were also used. Consequently, the chemistry of slags and other waste deposited in the vicinity of steel mills has changed.

3. Geological Background of the Sampling Area

In the area of Silesia and Kracow (Southern Poland), the Zn-Pb-Ag ore deposits are one of the largest in Europe and are classified as the MVT (Mississippi Valley-Type) [29]. The favourable geological and mining conditions of the deposits, representing the primary (hydrothermal) and secondary (supergene) types of mineralisation [4,5], favoured the development of Zn-Pb-Ag ore mining. The basement is upper Carboniferous sedimentary rocks, from which numerous underground mines have exploited hard coal for over 200 years.

In the area of the Bytom Basin, on the Carboniferous rocks, there are limestone-dolomitic sedimentary rocks of the Middle Triassic and clay formations of the Keuper. Residual weathering and fluvioglacial sands of Pleistocene age occur locally on the eroded, Triassic and Carboniferous deposits. Epigenetic ore-bearing dolomite with Zn-Pb-Ag deposits is located in the Middle Triassic horizons [24] (Figure 1). In the Silesian-Cracow area, most Zn-Pb ores bodies are located from 40 to 150 m below surface. However, locally, these ore bodies may be present on the surface as well. The deposits formed in the Cretaceous period [29]. After this period, the weathering of primary sulphides led to geochemical changes and the formation of supergene-type Zn-Pb-Fe deposits.

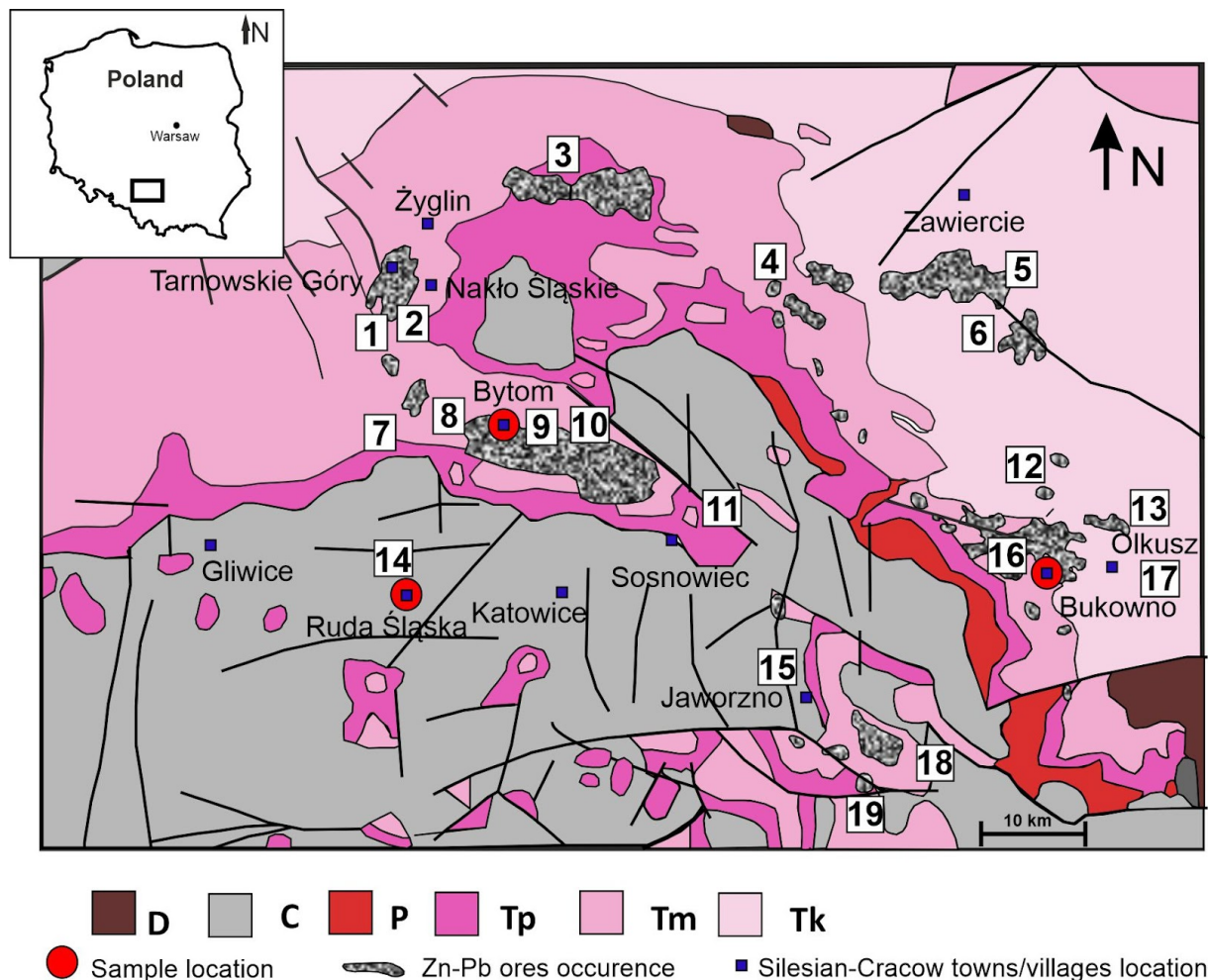


Figure 1. Simplified geological map of the investigated area, including the Zn-Pb ores occurrences. Explanations: D—Devonian, C—Carboniferous, P—Permian, Tp—Lower Triassic, Tm—Middle Triassic, Tk—Upper Triassic (Keuper), 1—Zn-Pb-Ag “Fryderyk” mine in Tarnowskie Góry, 2—flushing heap of the “Fryderyk” mine in Tarnowskie Góry, 3—Zn smelter in Miasteczko Śląskie, 4—Zn-Pb ores in Marciszów, Poręba, Siewierz, Gołuchowice, 5—Zn-Pb ores in Zawiercie I and Zawiercie II, 6—Zn-Pb ore Rodaki-Rokitno Szlacheckie, 7—dump in Bytom-Bobrek, 8—Zn “Bobrek” smelter, later a Fe smelter in Bytom, 9—dump in Bytom-Rozbark near the “Żabie Doły” reservoir, 10—Zn-Pb mine “Biały Szarlej” and ZGH “Orzeł Biały” in Piekary Śląskie, 11—Zn smelter “Paulina” in Sosnowiec, 12—Zn-Pb ores Chechło and Rudnica, 13—Zn-Pb mine “Pomorzany”, 14—metallurgical waste landfill, closed Zn smelters “Hugo”, “Franciszek”, and “Liebe-Hoffnung”, 15—Zn smelter “Józefina” in Jaworzno-Niedzieliska, 16—Mining and metallurgical works “Bolesław” in Bukowno, 17—a heap of post-flotation waste in Bolesław, 18—Zn-Pb smelter “Jadwiga” in Trzebinia, later metallurgical plants “Giesche” and “Trzebinia”; Zn smelter “Artur”, 19—mine of Pb ores “Matylda” in Chrzanów.

Primary ores are composed of simple Zn, Pb, Fe sulphides, and minor Cd, with which the following concentrations are related: Ag, As, Tl, Sb, Ba, and Ge. Silver, As, and Ta do not form minerals, accumulating in the crystal lattice of Zn-Pb-Fe sulphides. Oxidised ores (the supergene ore type) build Zn and Pb carbonates and Fe oxides and hydroxides accompanied by Zn oxides and silicates. Ca sulphates and unstable Mg, Fe, Zn, and Pb sulphates are also present in the weathering zones. Mineral components of the Silesian-Cracow Zn-Pb ores are listed in Table 1. In the Silesia and Cracow area, in regions affected by Zn and Pb mining and metallurgy, the primary sources of Zn, Pb, Ag, Cd, Tl, As, and Sb are Zn-Pb ores. The mineral composition of the ores is simple, and there are several generations of Zn (sphalerite-wurcite), Pb (galena), and Fe (pyrite-marcasite) sulphides [30,31]. The elements accompanying Zn-Pb ores are concentrated in different generations of Zn, Pb, and Fe sulphides [24,32].

Table 1. Minerals from the Zn-Pb-Ag ore deposits (Silesian-Cracow MVT). References: ¹—[33]; ²—[1]; ³—[34]; ⁴—[12]; ⁵—[35]; ⁶—[36]; ⁷—[2]; ⁸—[37].

Soil Areas Contaminated by Zn, Pb, Cd, As, Sb			
	Zn-Pb Ore Mining	Zn-Pb Ore Processing	Zn-Pb Smelting
Main gangue components	dolomite (CaMg[CO ₃] ₂) ^{2,3,5} calcite (CaCO ₃) ^{2,3,5} ankerite (Ca(Fe,Mg,Mn)(CO ₃) ₂) ² quartz (SiO ₂) ³ clay minerals ^{2,3}	quartz (SiO ₂) ¹ dolomite (CaMg[CO ₃] ₂) ^{1,2} calcite (CaCO ₃) ¹ ankerite (Ca(Fe,Mg,Mn)(CO ₃) ₂) ¹ illite (KAl ₂ (Si,Al) ₄ O ₁₀ (OH) ₂) ¹ montmorillonite (Al ₂ O ₃ ·SiO ₂ ·nH ₂ O) ¹ kaolinite (Al ₂ (OH) ₄ Si ₂ O ₅) ¹	quartz (SiO ₂) ^{4,7,8} cristobalite (SiO ₂) ^{4,8} trydymite (SiO ₂) ⁴ diopside (MgCaSi ₂ O ₆) ⁸ plagioclase ⁸ feldspar (e.g. anorthite) ⁴ mica ⁸ pyroxene ^{4,7} calcite (CaCO ₃) ^{7,8}
Primary metalliferous minerals	marcasite (FeS ₂) ^{3,5} pyrite (FeS ₂) ⁵ sphalerite ((Zn,Fe)S) ^{2,3,5} galena (PbS) ^{2,3,5}	marcasite (FeS ₂) ^{1,6} pyrite (FeS ₂) ^{1,6} sphalerite ((Zn,Fe)S) ¹ galena (PbS) ^{1,2}	sphalerite ((Zn,Fe)S) ⁸ wurtzite ((Zn,Fe)S) ⁸
Secondary metalliferous minerals	hemimorphite (Zn ₄ Si ₂ O ₇ (OH) ₂ ·H ₂ O) ^{2,3} smithsonite (ZnCO ₃) ^{2,3} minrecordite (CaZn(CO ₃) ₂) ² cerrusite (PbCO ₃) ^{2,5} barite (BaSO ₄) ² anglesite (PbSO ₄) ^{2,5} gypsum (CaSO ₄ ·2H ₂ O) ² jarosite (KFe ₃ (SO ₄) ₂ (OH) ₆) ² willemite (Zn ₂ SiO ₄) ⁵ goethite (FeO(OH)) ^{2,3} magnetite (Fe ₃ O ₄) ² Mn oxide ³ Fe hydroxide ²	alluminosilicates ^{1,2} minrecordite (CaZn(CO ₃) ₂) ² smithsonite (ZnCO ₃) ^{1,2} cerrusite (PbCO ₃) ^{1,2} Ca phosphates ² Mn-Fe, Mn oxides ^{1,2} Fe oxides ² goethite (FeO(OH)) ^{1,2} gypsum (CaSO ₄ ·2H ₂ O) ^{1,6} anglesite (PbSO ₄) ¹ bassanite (CaSO ₄ ·0.5H ₂ O) ^{1,6} jarosite (KFe ₃ [(OH) ₆ /(SO ₄) ₂]) ¹ epsomite (MgSO ₄ ·7H ₂ O) ^{1,6}	cerrusite (PbCO ₃) ^{2,7} barite (BaSO ₄) ^{2,8} gypsum (CaSO ₄ ·2H ₂ O) ⁷ litharge (PbO) ² alluminosilicates (e.g. mullite) ² Pb phosphates ² Pb arsenate ⁸ magnetite (Fe ₃ O ₄) ^{4,8} hematite (Fe ₂ O ₃) ^{7,8} goethite (FeO(OH)) ⁸ mullite (Al ₆ Si ₂ O ₁₃) ^{4,8} akermanite (Ca ₂ Mg(Si ₂ O ₇) ₇) ⁷ melilite (Ca,Na) ₂ (Al,Mg,Fe ²⁺) ⁷ willemite (Zn ₂ SiO ₄) ⁷ zircon (ZrSiO ₄) ⁸ Zn-Fe oxide/hydroxide ⁸ apatite (Ca ₅ (PO ₄) ₃ (F,Cl,OH)) ⁴ Fe oxide ⁷ franklinite (ZnFe ³⁺ 2O ₄) ⁴ zincite ((Zn,Mn)O) ⁴ birnessite ((Na,Ca) _{0.5} (Mn ⁴⁺ ,Mn ³⁺) ₂ O ₄ ·1.5H ₂ O) ⁸

4. Materials and Methods

The investigated samples, 33 soils and 12 slags, were taken from depths of 0.0–0.3 m. The symbols of samples can be found in Table S1. The sample mass from 0.25 m × 0.25 m was averaged and reduced to about 1 kg. The sampling locations are presented in Figure 1. One sample from each area was chosen for pH measurement.

4.1. Optical Microscopy and Scanning Electron Microscope (SEM)

Petrographic analyses of polished mounts (prepared from bulk soils) at the Institute of Earth Sciences, the University of Silesia in Katowice, using an Olympus BX-51 microscope, were undertaken to select representative samples for subsequent electron probe microanalysis (EPMA) and whole-rock major and trace element geochemical analyses. A ThermoFisher Scientific Phenom XL Scanning Electron Microscope (SEM) with back-scattered electron (BSE) imagery coupled with an energy dispersive spectrometer (EDS) was also applied to assist with the petrographic analyses.

4.2. Electron Probe Microanalysis (EPMA)

Microprobe analyses of the main and accessory minerals were carried out at the Inter-Institutional Laboratory of Microanalyses of Minerals and Synthetic Substances, University of Warsaw, using a CAMECA SX-100 electron microprobe, manufactured by CAMECA SAS France. The analytical conditions were as follows: an acceleration voltage of 15 kV, beam current of 20 nA, counting time of 4 s for peak and background, a beam diameter of 1–5 mm, a peak count-time of 20 s, and a background time of 10 s. Standards, analytical lines, diffracting crystals, and mean detection limits (in wt%) were as follows: rutile—Ti ($K\alpha$, PET, 0.03), diopside—Mg ($K\alpha$, TAP, 0.02), orthoclase—Al ($K\alpha$, TAP, 0.02), Si—($K\alpha$, TAP, 0.02) and K ($K\alpha$, PET, 0.03), albite—Na ($K\alpha$, TAP, 0.01), wollastonite—Ca ($K\alpha$, PET, 0.03), hematite—Fe ($K\alpha$, LIF, 0.09), rodohrozite—Mn ($K\beta$, LIF, 0.03), phlogophite—F ($K\alpha$, TAP, 0.04), tugtupite—Cl ($K\alpha$, PET, 0.02), Cr_2O_3 —Cr ($K\alpha$, PET, 0.04), ZirconED2—Zr ($L\alpha$, PET, 0.01), Nb_2O_3 -MAC—Nb ($L\alpha$, PET, 0.09), and V_2O_5 —V ($K\alpha$, LIF, 0.02).

4.3. ICP-ES/MS

The most homogeneous parts of the samples were selected for whole-rock geochemistry. The samples were first crushed using a jaw crusher and pulverised in an agate ball mill to a fine-grained powder. The material was then coned and quartered before being despatched for major and trace elements analysis in the Bureau Veritas Analytical Laboratories in Vancouver, Canada. Approximately 0.25 g of each sample was digested using the so-called four-acid method ($HF + HClO_4 + HCl + HNO_3$) with the use of thermal conductivity. In such prepared solutions, the content of elements was analysed by ICP-ES (emission spectrometry with excitation in an induced plasma) or ICP-MS (inductively coupled plasma mass spectrometry) depending on the concentration of elements in the samples. The quality control of the instrumental measurements was confirmed by blank analysis, duplicate samples, and the use of the standard internal reference material (OREAS25A-4A and STD OREAS45E). The results are presented in Table S1. All obtained concentrations of the elements were normalised to sample B4(S), collected from the Bobrek area. The lowest content of heavy metals characterises the sample, including, for example, Cd, Pb, Zn, As, and Sb. It represents glacial sand with minor clay material (typical of the soil in the area).

4.4. pH

This was measured using an Elmetron CP-401 pH meter in distilled (boiled) water. For pH determination, water extracts of soil samples were prepared by pouring 10 g of a sample with 25 mL of deionised water and left to stand for three hours according to the Polish Standard.

5. Results

5.1. Mineral Components

All topsoil samples are highly weathered. Their form and physical properties indicate strong development of oxidation processes in interaction with soil solutions, probably from microorganisms and fungi. Most samples are orange, yellow, slightly pink, or pale brown. Moreover, almost all of them are composed of fine-grained, loose material. Macroscopically, the mineralogical composition is difficult to recognise.

The measured pH values of the topsoil samples were in the range of 5.86 to 10.12. Samples from Bytom-Żabie Doły and Ruda Śląska were acidic (5.86 and 6.06, respectively), while in the galmanic areas in Bolesław and Bytom-Bobrek, they were basic (7.96 and 10.12, respectively). EPMA revealed that almost 80% of the investigated material is represented by oxides and hydroxyl oxides of Fe, most probably from goethite and limonite. Dolomite is greater than calcite; quartz and aluminosilicates (clay minerals) are the main components of the soil. In the whole mineral suite, two different groups are distinguished. They are represented by

- (1) primary, fresh, or partially decomposed ore minerals (Zn-Pb-Fe sulphides and their accessories);
- (2) secondary phases formed in the soil environment;
- (3) synthetic phases resulting from smelting processes.

5.1.1. Primary Phases

The first group is mainly composed of the most typical Zn-Pb-Fe ore minerals, including galena, sphalerite, and iron sulphides (pyrite/marcasite). In most cases, the primary minerals are overgrown by secondary phases, starting with slightly oxidised ones, close to the contact, and strongly changed in the outer zone. The average size for this last group does not exceed 200 µm in diameter.

Non-oxidised galena from the investigated topsoil is characterised by the typical chemical composition, where trace elements were also noted (Table 2). Some potentially toxic elements (at.%) as Se, Sb, and Cd are up to (wt%) 0.21, 0.76, and 0.28, respectively. Oxidation-affected galena grains are depleted in the same trace elements (Table 2). Anglesite and cerussite commonly crystallise on galena. This relationship is typical of all topsoil studied.

Table 2. Representative electron microprobe analysis (EMPA) of sulphides from the investigated samples. Elemental content in wt%; b.d.l.—below detection limit; SD—standard deviation; n—number of analyses.

Mineral/ Compound	Galena (n = 25)				Sphalerite (n = 19)				Pyrite/Marcasite (n = 34)			
	Min	Max	Average	SD	Min	Max	Average	SD	Min	Max	Average	SD
Fe	0.20	0.54	0.42	0.13	0.08	0.09	0.08	0.01	46.80	47.30	47.11	0.16
Ni	0.11	0.26	0.19	0.08		b.d.l.				b.d.l.		
Cu	0.08	0.09	0.09	0.01		b.d.l.				b.d.l.		
Zn	0.09	0.43	0.22	0.12	66.17	67.15	66.67	0.25	0.08	0.11	0.10	0.02
Se	0.10	0.21	0.16	0.06		b.d.l.				b.d.l.		
Pb	79.90	86.71	84.92	1.64	0.10	0.15	0.12	0.02	0.10	0.13	0.12	0.02
Sb	0.21	0.76	0.36	0.19		b.d.l.				b.d.l.		
Cd	0.12	0.28	0.20	0.07		b.d.l.				b.d.l.		
As		b.d.l.				b.d.l.			0.06	0.11	0.08	0.02
S	11.88	13.84	13.47	0.45	32.47	33.13	32.71	0.16	52.94	54.02	53.61	0.28
Total			99.87				99.43				100.77	

Among the studied samples and zinc sulphides, sphalerite occurs as isolated, often euhedral or massive grains or aggregates with dispersed very fine grained pyrite/marcasite zones (Figure 2A). The sphalerite grains/aggregates are up to 100 µm in size and are homogenous in chemistry. This phase is the most common primary phase in the sample from the Olkusz area. Only Fe and Pb substitution was noted in the sphalerite, up to 0.09 wt% and 0.15 wt%, respectively. The typical composition of sphalerite is shown in Table 2.

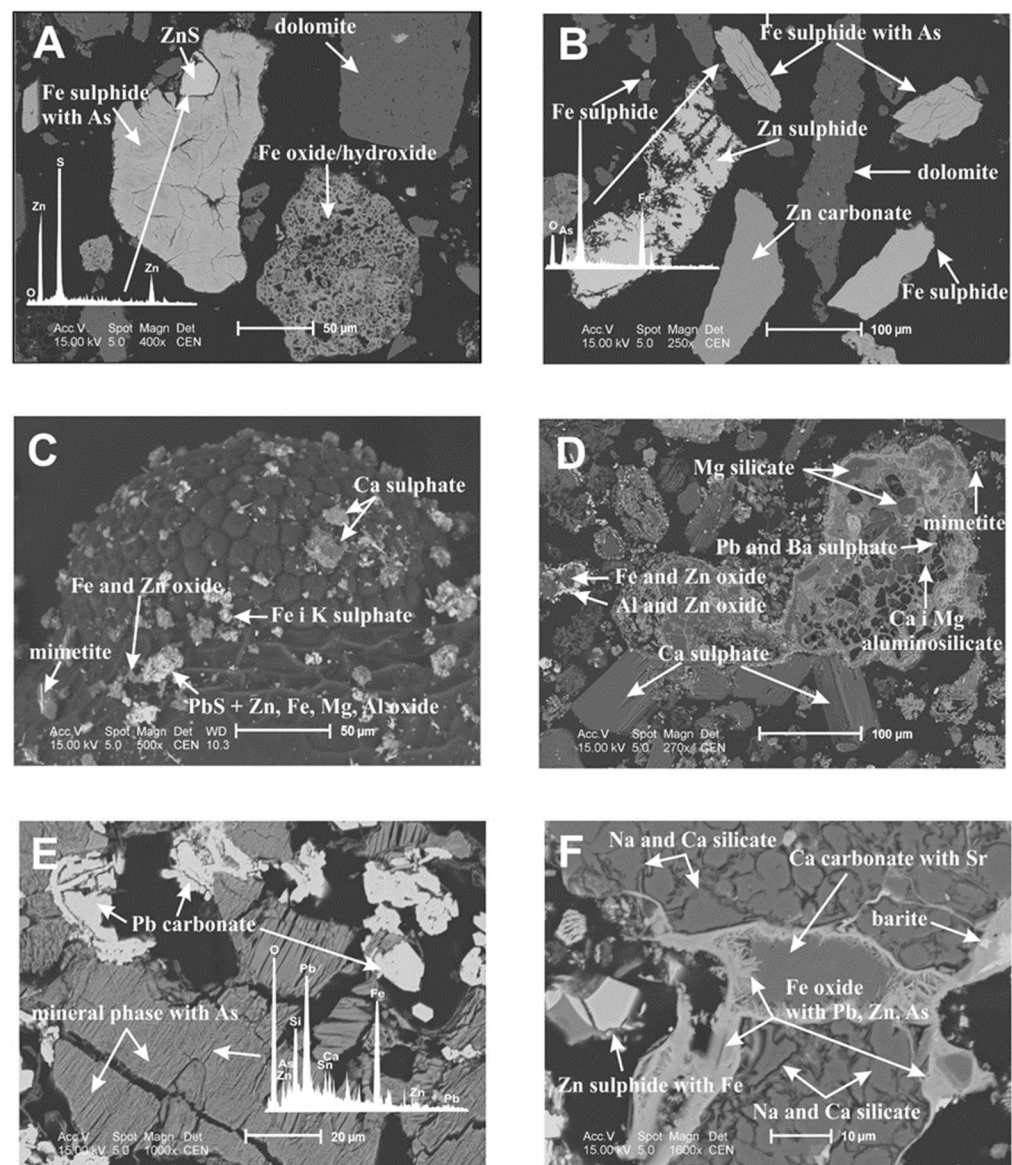


Figure 2. Selected BSE images and EDS spectra of minerals from the galmanic topsoil from the Silesia region. Explanations: (A,B)—ZD11 (Bytom-Żabie Doły) soil sample, EDS spectra of Zn sulphide; (C,D)—R1 (Ruda Śląska) soil sample; (E,F)—B2 (Bytom-Bobrek) soil sample, EDS spectrum of mineral phase with As.

Iron sulphides mainly occur as fine-crystalline aggregates in which marcasite dominates over pyrite. The Fe sulphides are microporous, often accompanied by Ca sulphates (Figure 3D). In their microareas, Zn up to 0.11 wt% and Pb up to 0.13 wt% have been identified in EDS spectra (Table 2). Fine-crystalline Fe sulphides in topsoil enriched in synthetic phases from Zn-Pb metallurgy are characterised by arsenic up to 0.11 wt% (Table 2; Figures 2A,B and 3D).

The studied topsoil contains barite grains. The crystals are platy, ranging from a few to 100 µm in size (Figures 2F and 3C). Barite is associated with Zn-Pb carbonates and Zn-Pb-Fe sulphides (Figures 2F and 3C). Isolated barite grains are present in the non-contaminated topsoil with Zn-Pb slag content. However, in aggregates derived from metallurgical processes, barite is commonly melted and associated with the Na-Ca glass (Figure 2F).

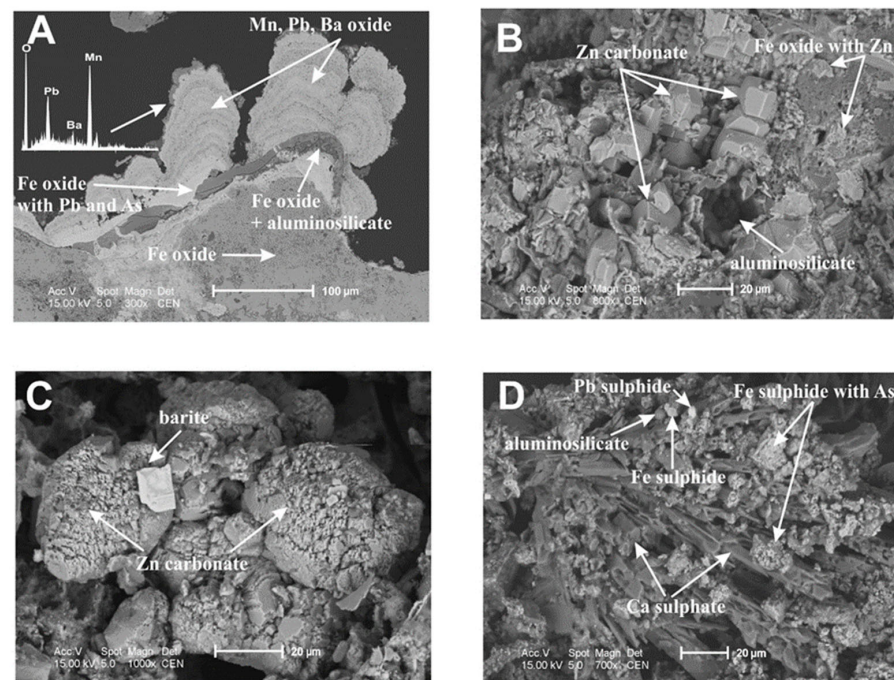


Figure 3. Selected BSE images and EDS spectra of minerals from the galmanic topsoil from the Olkusz region. Explanations: (A–C)—TP1 (Bukowno) soil sample; (D)—TP3 (Bukowno) soil sample (slag).

5.1.2. Secondary Phases

Secondary minerals formed due to the weathering of the primary ore phases are represented mainly by carbonates, sulphates, and, rarely, silicates. This group of minerals can be divided into two subgroups formed directly at the deposit site and into minerals formed at their surface (Figure 4A–D). Regardless of where they originate, these minerals are similar in chemical composition. The most common minerals in this group are cerussite, smithsonite, gypsum, anglesite, jarosite, pyromorphite, and hemimorphite. They are commonly associated with barite, goethite, and Mn-Fe oxides (Figure 4A,C).

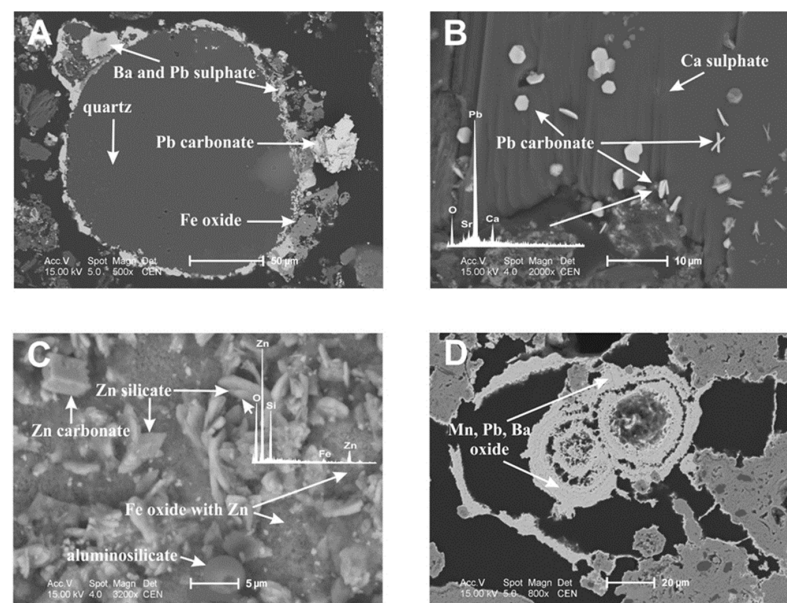


Figure 4. Selected BSE images and EDS spectra of minerals from the galmanic topsoil from the Ruda Śląska and Olkusz regions. Explanations: (A,B)—R1 (Ruda Śląska) soil sample; EDS spectra of Pb carbonate; (C,D)—TP1 (Bukowno) soil sample; EDS spectra of Zn silicate.

The most common sulphates are Ca (gypsum) and Pb (anglesite). Ca sulphates form automorphic to hipauthomorphic crystals, overgrowing pyrite/marcasite zones (Figure 3D). Pb sulphide (anglesite) occurs in the form of dispersed, submicroscopic grains, which EPMA methods can identify. Anglesite forms colomorphous forms in the studied samples. It is homogenous in form, where Fe > Zn > Mn substitution is observed (Table 3).

Table 3. Representative electron microprobe analysis (EMPA) of carbonates, sulphates, and phosphates from the investigated samples. Chemical constituents in wt%; b.d.l.—below detection limit; n.a.—not analysed; SD—standard deviation.

Mineral/ Compound	Smithsonite (n = 13)				Barite (n = 9)				Anglesite (n = 15)				Pyromorphite (n = 12)				Mimetite (n = 1)
	Min	Max	Avg	SD	Min	Max	Avg	SD	Min	Max	Avg	SD	Min	Max	Avg	SD	
Cl		n.a.				n.a.				n.a.			2.49	2.74	2.65	0.08	2.26
Na ₂ O		n.a.			0.09	0.13	0.11	0.02		n.a.				n.a.			n.a.
CaO	0.92	1.60	1.35	0.19	0.00	0.19	0.08	0.07		n.a.			0.22	0.61	0.40	0.14	0.31
MnO	0.10	0.13	0.10	0.02					0.00	0.06	0.02	0.02		b.d.l.			b.d.l.
SrO		b.d.l.			0.10	0.20	0.14	0.04	0.00	0.05	0.01	0.01		n.a.			n.a.
BaO		b.d.l.			65.91	68.35	67.59	0.99	0.00	0.26	0.06	0.08		n.a.			n.a.
Fe ₂ O ₃		n.a.			0.10	0.30	0.17	0.08					0.00	0.40	0.10	0.12	0.11
FeO	0.23	0.49	0.35	0.07		n.a.				n.a.				n.a.			n.a.
ZnO	59.32	62.91	61.47	1.14		n.a.			0.13	0.43	0.21	0.11		b.d.l.			n.a.
As ₂ O ₃		b.d.l.				b.d.l.							0.00	0.14	0.06	0.05	19.51
CdO		b.d.l.				b.d.l.			0.05	0.49	0.31	0.19		b.d.l.			b.d.l.
Sb ₂ O ₃		b.d.l.				b.d.l.			0.10	0.10	0.10	0.00		b.d.l.			b.d.l.
PbO	0.10	0.25	0.18	0.06		b.d.l.			72.80	73.94	73.36	0.35	78.34	81.69	80.10	1.08	75.11
SiO ₂	0.13	0.26	0.20	0.05		n.a.				n.a.			0.00	0.97	0.33	0.33	0.69
Al ₂ O ₃		n.a.				n.a.				n.a.			0.00	0.40	0.14	0.14	b.d.l.
P ₂ O ₅		b.d.l.				n.a.				n.a.			14.97	15.55	15.29	0.18	0.34
SO ₃	0.07	0.07	0.07	0.00	32.85	34.76	33.51	0.76	26.26	27.36	26.65	0.27		n.a.			n.a.
CO ₂	35.35	38.51	36.82	0.95		n.a.				n.a.				n.a.			n.a.
Total			100.00				101.61				100.29				99.57		98.33

The Fe and Mn (hydro)oxides form colomorphous forms or thin films overgrowing other phases. They are present in nearly all studied localities. Based on EDS, most of them are similar in composition to Fe (hydro)oxides and Mn-Fe oxides aggregates. Some of them revealed the presence of Pb, As, and Ba (Figure 3A,B; Table S3).

Pyromorphite (phosphate) was only found in the Bytom-Żabie Doły area. The crystals are short to long prismatic, up to 70 µm in length. Occasionally, amoeba-like forms were also noted. The chemical composition shows slight enrichments in As and Cl (see Table 3). In Ruda Śląska and Bytom-Bobrek, other minerals were found, and crystal morphology and analysis of EDS spectra indicate that it is probably mimetite (Figure 2C,D). Moreover, Si-Ca aggregates with metals, including As (Figure 2E), were observed. These aggregates are found in post-metallurgical products (slags).

In the Olkusz area, one unusual phase was found. It is selenide (?) with a high, up to 45.11 wt% content of Ag (see Table 4). It forms aggregates up to 200 µm in length which seems to be a pseudomorph. The chemical composition is shown in Table 4.

Table 4. Representative electron microprobe analysis (EMPA) of Se and Ag phases from the Olkusz area. Elemental content in wt%.

Compound	an.1	an.2	an.3	an.4	an.5	an.6	an.7	an.8	an.9	an.10	an.11	an.12
Fe	0.32	0.36	0.26	0.41	0.17	0.53	0.30	0.25	0.27	1.21	1.30	1.85
Zn	0.22	0.17	b.d.1	0.20	b.d.1	0.15	0.19	b.d.1	b.d.1	0.10	0.18	0.20
Se	16.55	17.37	18.12	19.50	21.96	16.66	18.47	9.83	17.40	2.04	3.98	4.39
Pb	20.48	61.30	28.60	23.62	27.44	33.21	65.44	45.20	64.54	70.18	69.93	68.08
Ag	34.59	3.43	26.43	45.11	42.14	23.06	0.82	0.70	0.93	b.d.1	0.27	0.12
S	2.34	3.44	2.77	2.01	1.82	2.94	3.90	2.47	4.04	9.91	9.30	9.41
Total	74.50	86.09	76.17	90.85	93.56	76.55	89.15	58.44	87.18	83.50	84.97	84.08
Crystal chemical formulae recalculated on the basis of 2 Se ²⁻	Crystal chemical formulae recalculated on the basis of sum (Se ²⁻ + S ²⁻) ₁											
Fe	0.06	0.02	0.01	0.02	0.01	0.03	0.02	0.02	0.01	0.06	0.07	0.09
Zn	0.04	0.01		0.01		0.01	0.01				0.01	0.01
Pb	0.94	0.90	0.44	0.37	0.40	0.53	0.89	1.08	0.90	1.01	0.99	0.94
Ag	2.06	0.10	0.78	1.35	1.17	0.71	0.02	0.03	0.02		0.01	0.00
S	1.05	0.33	0.27	0.20	0.17	0.30	0.34	0.38	0.36	0.92	0.85	0.84
Se	2.00	0.67	0.73	0.80	0.83	0.70	0.66	0.62	0.64	0.08	0.15	0.16

6. Discussion

6.1. The Natural Content of PHEs in Topsoil

The limit of the heavy metal concentration in ordinary soil is <1000 ppm. Based on this, almost all investigated samples are contaminated by PHEs. The average PHE (Zn, Pb, Cd, Tl) content is 36,732 ppm, and metalloids (As, Sb, Se) are 4747 ppm (see Table S1). Based on the presented heavy metal pollution definition, all investigated sites (samples) are highly polluted by heavy metals (excluding the B4(S) sample). The diversity of the mineral components of soils affected by Zn-Pb metallurgy is very high. Not only were minerals typical of Zn-Pb deposits identified, but also metal-bearing phases containing, among other elements, Cu and Sn, which are strongly associated with the contamination of the Upper Silesian region (Table S2). The samples show visible enrichment of Zn, As, Se, Cd, Sb, and Pb (Tables 2, 4, and S1), which is higher than the other analysed heavy metals (Table S1). In all cases (excluding the sample used for normalisation), Pb dominates over the other elements.

6.2. Distribution of Selected PHEs in the Topsoil

Potentially harmful elements (i.e., Cd, Pb, Tl, Zn, As, Sb) found in soils developed on slags or post-mining waste may significantly increase bioavailability in synergy with humic and fulvic acid, root exudates, microbial metabolites, and nutrients [38]. The presence of active organic compounds complicates the geochemistry of these environments. Unstable, organometallic phases with Pb, Zn, Cd, and Mn are formed in mycorrhised rhizospheres contaminated with minerals from mining and Zn-Pb metallurgy [39,40]. The complex of ore minerals and mineral paragenesis identified in the studied soils is similar to the one described above (Table 2).

In zinc sulphides from the Olkusz region, Cd concentrations were 2700 ppm [41]. Harańczyk [30], in Zn sulphides from Bytom deposits, indicated Cd concentrations ranging from 1000 to 5000 ppm. Concentrations up to 10,000 ppm have been reported in sphalerites [24,32]. In the weathering Zn-Pb ore stages, Zn from Cd geochemical separation occurs. Cadmium, depending on environmental conditions, enters the structure of Zn carbonate (smithsonite), forming Cd carbonate (ottavite) or secondary sulphide (greenockite) [5,42,43]. Historical slags after Zn production in Świętochłowice (southern Poland) contain over 500 ppm of Cd. A significant part of Cd in metallurgical processes passes to the

slag-building phases [11]. EPMA analyses show this element is also located in galena and anglesite (Tables 2 and 3). Silesia-Kracow Zn-Pb ores are rich in iron sulphides (marcasite and pyrite), and the As contents in these minerals were very high and could reach up to 20,000 ppm [18]. Viets et al. (1996) [24], in Fe and Pb sulphides, report As concentrations up to 10,000 ppm. Mikulski et al. (2020) [35] determined the average As content in Fe sulphides with a high variability of 2237 ppm and the maximum at 26,950 ppm.

No silver minerals have been identified in the Silesia-Kracow Zn-Pb ore deposits. High concentrations of this metal occur in galena. However, Viets et al. (1996) [24] indicated significant (up to 300 ppm) Ag concentrations in a dark blende (ZnS) species. Ag contents in galena and sphalerites are similar and variable, ranging from 100 to 1000 ppm [35]. Contemporary research has not confirmed information from historical sources that the concentration of Ag in some galena from the Silesia-Kracow deposits reaches 1% (10,000 ppm). Keim et al. (2016) [44] indicated that Ag scattering occurs in weathering Ag-bearing galena. Cerussite and anglesite are mostly Ag free. Based on the above, the Ag released during weathering of argentiferous galena is likely to be removed as soluble ions/complexes or reprecipitated as distinct Ag phases. The dispersion of Ag under the conditions of hypergenesis may explain the lack of Ag minerals and the secondary depletion in this metal in waste from the mining and metallurgy of Zn-Pb ores. It is, therefore, important to identify submicroscopic mineral phases representing silver selenides (Table 4). Se and Ag were found in the examined soil samples (Table S1) and selected minerals. Selenium and Ag are elements mostly in galena. It is possible that under specific oxidation conditions, secondary Pb-Ag-Se phases could form. This association, during soil weathering, may be responsible for the secondary demobilisation of Se and S in oxidation processes of Ag-rich galena for such phases. The presence of pyromorphite is probably related to the secondary distribution of P and Cl. These elements indicate that Pb^{2+} ions activated in the environment are stabilised in the pyromorphites. Phosphorus contents in some samples are relatively high and reach up to 0.339% in R4 from Ruda Śląska and from 0.123 up to 0.218% in TP9 and TP10 samples from Bukowno (Table S1). The presence of pyromorphite proves a local stabilisation of Pb ions in soils.

6.3. Mineral Changes and PHE Migrations

The Fe sulphide aggregates present in the investigated soils can be easily dissolved and are a source of sulphate ions and Zn, Pb, As, and Sb ions. Acid waste drainage (AWD) can be stimulated under acidified soil conditions by organics or acid rainfall [36,37]. The high proportion of unstable Zn and Fe sulphides significantly increases the environmental risk of increasing the pool of bioavailable HMs. A more stable and environmentally non-hazardous mineral is Ba sulphate. Barite mineralisation is primarily a characteristic of the Silesia-Kracow Zn-Pb ores [5,24]. The presence of barite in associations with Zn and Pb carbonates and Fe oxides is associated with the enrichment processes of Zn-Pb ores in which unsuitable and heavy barite is separated into waste together with carbonates and Zn and Pb, Fe oxides, and clay minerals. Furthermore, the studied soils are contaminated with wastes deposited in the areas around mines and steel mills.

In soils from Ruda Śląska and Bytom-Bobrek, numerous mimetite crystals (1 to 20 μm in length) were identified (Figure 2C,D). This mineral is most often formed in the final stages of the transformation of Pb arsenates [45], commonly described as a secondary mineral in the oxidation zone of Pb-As deposits [46,47] and in the weathering of slags [48]. Arsenic and Pb minerals are relatively numerous but, in nature, are rare [49]. It is a relatively insoluble and thermodynamically stable mineral, particularly at a $\text{pH} > 5$ [50]. The mobility and bioavailability of As and Pb can be controlled by mimetite crystallisation [51–53]. Arsenic is mobilised into the environment by weathering As-rich Fe sulphides (Table 2). It does not always diffuse into the environment. The stability of mimetite decreases at low pH and in the presence of organic acids. Mimetite, together with isostructural vanadinite $Pb_5(VO_4)_3Cl$ and pyromorphite $Pb_5(PO_4)_3Cl$, can crystallise in the oxidation zone of Pb-bearing ores [53,54]. Arsenic up to 1000 ppm is also concentrated in pyromorphite (Table 3). Moreover, pyro-

morphite and mimetite have similar thermodynamic properties [53]. Both mimetite and pyromorphite contain Cl. This element is dispersed in ore minerals from the Silesia-Kracow deposits, and therefore dechlorination is necessary for technological purification processes. Mimetite formation is possible when one of the components is present in the adsorbed form of goethite [52]. Si-Ca aggregates with Fe, Pb, Sn, Zn, and As were also frequently identified in the investigated soils (Figure 2E). The geochemical composition of these aggregates and the grain morphology seen in the BSE images (Figure 4C) indicate their metallurgical origin.

Soil pH has a significant influence on many (bio) chemical processes occurring in the soil [55–57]. The soil reaction affects the leachability of elements from mineral phases and determines the pool of bioavailable macro- (K, Ca, Mg, P, S) and microelements (Fe, Mn, Cu, Zn, Mo). They are necessary for the proper growth of plants and the functioning of microorganisms [58]. The pH range indicates the quality of soils and also suggests the possibility of their degradation, especially at low (<4.5) pH values [59]. The tested soil shows an alkaline reaction in the Silesia-Kracow Zn-Pb ore region in the galmanic areas. These soils are formed on Triassic carbonate formations (dolomites or limestones) and waste from the washing, flotation, or smelting of Zn-Pb-Ag ores. The mineral composition of Zn-Pb ores and waste remaining after enrichment has a decisive influence on the relatively high pH [18]. This has the advantage of hindering the leaching of heavy metals and their further transfer to plant tissues. Among the studied soils, the soil from Bytom-Bobrek is significant for its strongly alkaline reaction (pH > 10). Microscopic studies indicate the presence of significant amounts of waste from Zn smelters. Si-Ca aggregates with the metal characteristic of slags were also identified. Similar to coal combustion ash, smelter waste is characterised by a high pH [60,61]. The atmospheric deposition of combustion products from high and low emissions can also have a significant impact.

The most significant risk of plant uptake of large amounts of PHEs (i.e., Cd, Pb, Zn) and metalloids (As, Sb) is marked in the area of Ruda Śląska and Bytom-Żabie Doły. This is due to the relatively low pH of the soils. Identified high concentrations of PHEs pose a risk of the transfer of ions from these metals to water and living organisms. Some elements (Zn, Cd), with minor changes in soil chemistry, can be easily precipitated and/or adsorbed by mineral phases or organic matter [62]. Soils from the area of Ruda Śląska and Bytom-Żabie Doły have an acid reaction, which in Ruda Śląska can be associated with the presence of lead sulphides and Ca sulphates (Figure 2C,D), and in Bytom-Żabie Doły, with unstable Fe and Zn sulphides (Figure 2A,B), which in oxidation processes are a source of sulphate ions that can significantly reduce soil pH. The presence of Ca (gypsum) sulphates indicates sulphur leaching in the form of SO_4^{2-} ions, which are buffered in the presence of Ca^{2+} ions in the form of sulphates. The mass oxidation of sulphides under conditions of Ca^{2+} ion deficit can lead to a significant reduction in pH and the formation of local acidic waste drainage conditions. These conditions promote further leaching of other HMs from the mineral phases in these soils/waste. In waste rich in metal sulphides (Fe, Zn, Cu) under temperate climate conditions, acid drainage develops, and severe environmental pollution occurs [63,64].

7. Conclusions

1. In Upper Silesia, high concentrations of Zn (above 10,000 ppm), Pb (above 10,000 ppm), and Cd (above 50 ppm) are found in topsoil around former Zn smelters (from the 19th and early 20th centuries). In some locations, concentrations of Cu (up to 9345 ppm) and Sn (up to 10,000 ppm) make it possible to identify sites of former alloy (e.g., bronze) and non-ferrous metal production.
2. The characteristic geochemical tracers for the studied soils are As, Sb, and Sr; the sources of As (from 1756 to more than 10,000 ppm) and Sb (from 106 to more than 4000 ppm) are Fe minerals. The final product of the geochemical transformations of As is mimetite. In contrast, Sr (125 to 4658 ppm) is mainly bound in Ca carbonates.
3. More than 120 years after the end of Zn-Pb smelters, soils still contain unstable Zn, Pb, and Fe sulphides, often rich in Cd, As, and Sb. Under favourable environmental

conditions, these minerals can be a source of ions, Pb^{2+} , Zn^{2+} , Cd^{2+} , Tl^{3+} , and AsO_3^{3-} , readily transferred to the aquatic and biotic environment. In addition, there is evidence of the periodic activation of ions Pb^{2+} , Zn^{2+} , Cd^{2+} , and SO_4^{2-} present in soils of oxidised phases such as anglesite (PbSO_4), mimetite $\text{Pb}_5(\text{AsO}_4)_3\text{Cl}$, pyromorphite ($\text{Pb}_5(\text{PO}_4)_3\text{Cl}$), smithsonite (ZnCO_3), hemimorphite ($\text{Zn}_4\text{Si}_2\text{O}_7(\text{OH})_2 \cdot \text{H}_2\text{O}$), jarosite ($\text{KFe}_3(\text{SO}_4)_2(\text{OH})_6$), and gypsum ($\text{CaSO}_4 \cdot 2\text{H}_2\text{O}$).

- ICP-ES/MS studies of soils contaminated by metal ore metallurgy made it possible to assess the total HM content; using SEM/EDS studies, it was possible to assess the size, morphology, and chemistry of the microareas. Meanwhile, EPMA made it possible to study and identify phases rich in As, Se, Sb, and Ag, that is, those that affect the total content of these metals.

Supplementary Materials: The following supporting information can be downloaded at <https://www.mdpi.com/article/10.3390/min14050475/s1>, Table S1: Element concentration in the studies samples (ICP-MS), Table S2: Minerals and mineral phases in studied soils and slags, Table S3: Minerals and mineral phases in studied soils and slags.

Author Contributions: Conceptualization, W.N., J.C. and K.S.; sampling of soils and slags and material preparation, W.N. and J.C.; SEM-EDS investigation and interpretation, W.N. and J.C.; EPMA analysis and interpretation, K.S.; geochemical data interpretation, W.N., J.C. and K.S.; data visualisation, W.N. and K.S. All authors have read and agreed to the published version of the manuscript.

Funding: The authors acknowledge the financial support from the Institute of Earth Sciences, Faculty of Natural Sciences, University of Silesia in Katowice, Poland.

Data Availability Statement: The data presented in this study are available on request from the corresponding author.

Acknowledgments: The authors thank Ashley P. Gumsley for his help in improving the English of the manuscript. The manuscript benefited from the comments of anonymous reviewers. The authors are very grateful for their work.

Conflicts of Interest: The authors declare no conflict of interest.

References

- Cabała, J.; Warchulski, R.; Rozmus, D.; Środek, D.; Szełęg, E. Pb-Rich Slags, Minerals, and Pollution Resulted from a Medieval Ag-Pb Smelting and Mining Operation in the Silesian-Cracovian Region (Southern Poland). *Minerals* **2020**, *10*, 28. [[CrossRef](#)]
- Tyszka, R.; Kierczak, J.; Pietranik, A.; Ettlér, V.; Mihaljevič, M. Extensive weathering of zinc smelting slag in a heap in Upper Silesia (Poland): Potential environmental risks posed by mechanical disturbance of slag deposits. *Appl. Geochem.* **2014**, *40*, 70–81. [[CrossRef](#)]
- Warchulski, R.; Gaweda, A.; Kadziółka-Gawel, M.; Szopa, K. Composition and element mobilization in pyrometallurgical slags from the Orzeł Biały smelting plant in the Bytom-Piekary Śląskie area, Poland. *Mineral. Mag.* **2015**, *79*, 459–483. [[CrossRef](#)]
- Boni, M.; Large, D. Nonsulfide zinc mineralization in Europe: An overview. *Econ. Geol.* **2003**, *98*, 715–729. [[CrossRef](#)]
- Cabala, J. Development of oxidation in Zn-Pb deposits in Olkusz area. In *Mineral Deposits at the Beginning of the 21st Century*; Piestrzyński, A., Ed.; Balkema: Lisse, The Netherlands, 2001; pp. 121–124.
- Vanaecker, M.; Courtin-Nomade, A.; Bril, H.; Laureyns, J.; Lenain, J.F. Behavior of Zn-bearing phases in base metal slag from France and Poland: A mineralogical approach for environmental purposes. *J. Geochem. Explor.* **2014**, *136*, 1–13. [[CrossRef](#)]
- Navarro, A.; Cardellach, E.; Mendoza, J.L.; Corbella, M.; Domènech, L.M. Metal mobilization from base-metal smelting slag dumps in Sierra Almagrera (Almería, Spain). *Appl. Geochem.* **2008**, *23*, 895–913. [[CrossRef](#)]
- Bevandić, S.; Blannin, R.; Vander Auwera, J.; Delmelle, N.; Caterina, D.; Nguyen, F.; Muchez, P. Geochemical and Mineralogical Characterisation of Historic Zn–Pb Mine Waste, Plombières, East Belgium. *Minerals* **2021**, *11*, 28. [[CrossRef](#)]
- Scheinert, M.; Kupsch, H.; Bletz, B. Geochemical investigations of slags from the historical smelting in Freiberg, Erzgebirge (Germany). *Chem. Der Erde-Geochem.* **2009**, *69*, 81–90. [[CrossRef](#)]
- Veselská, V.; Majzlan, J. Environmental impact and potential utilization of historical Cu-Fe-Co slags. *Environ. Sci. Pollut. Res.* **2016**, *23*, 7308–7323.
- Tyszka, R.; Pietranik, A.; Kierczak, J.; Zieliński, G.; Darling, J. Cadmium distribution in Pb-Zn slags from Upper Silesia, Poland: Implications for cadmium mobility from slag phases to the environment. *J. Geochem. Explor.* **2018**, *186*, 215–224. [[CrossRef](#)]
- Kupczak, K.; Warchulski, R.; Dulski, M.; Środek, D. Chemical and Phase Reactions on the Contact between Refractory Materials and Slags, a Case from the 19th Century Zn-Pb Smelter in Ruda Śląska, Poland. *Minerals* **2020**, *10*, 1006. [[CrossRef](#)]

13. Kasemodel, M.C.; Lima, J.Z.; Sakamoto, I.K.; Amancio Varesche, M.B.; Trofino, J.C.; Rodrigues, V.G.S. Soil contamination assessment for Pb, Zn and Cd in a slag disposal area using the integration of geochemical and microbiological data. *Environ. Monit. Assess.* **2016**, *188*, 698. [[CrossRef](#)] [[PubMed](#)]
14. Kondracka, M.; Cabała, J.; Idziak, A.; Ignatiuk, D.; Bielicka-Gieldoń, A.; Stan-Kłeczek, I. Detection of land degradation caused by historical Zn-Pb mining using electrical resistivity tomography. *Land Degrad. Dev.* **2021**, *32*, 3296–3314. [[CrossRef](#)]
15. Degryse, F.; Smolders, E. Mobility of Cd and Zn in polluted and unpolluted Spodosols. *Eur. J. Soil Sci.* **2006**, *57*, 122–133. [[CrossRef](#)]
16. Maskall, J.; Whitehead, K.; Gee, C.; Thornton, I. Long-Term Migration of Metals at Historical Smelting Sites. *Appl. Geochem.* **1996**, *11*, 43–51. [[CrossRef](#)]
17. Bănăduc, D.; Curtean-Bănăduc, A.; Cianfaglione, K.; Akeroyd, J.R.; Cioca, L.-I. Proposed Environmental Risk Management Elements in a Carpathian Valley Basin, within the Roşia Montană European Historical Mining Area. *Int. J. Environ. Res. Public Health* **2021**, *18*, 4565. [[CrossRef](#)] [[PubMed](#)]
18. Cabała, J. *Heavy Metals in Ground Soil Environment of the Olkusz Area of Zn-Pb Ore Exploitation*; University of Silesia: Katowice, Poland, 2009; Volume 2729, p. 127. (In Polish)
19. Chrastný, V.; Vaněk, A.; Teper, L.; Cabala, J.; Procházka, J.; Pechar, L.; Drahot, P.; Penížek, V.; Komárek, M.; Novák, M. Geochemical position of Pb, Zn and Cd in soils near the Olkusz mine/smelter, South Poland: Effects of land use, type of contamination and distance from pollution source. *Environ. Monit. Assess.* **2012**, *184*, 2517–2536. [[CrossRef](#)] [[PubMed](#)]
20. Ettler, V.; Červinka, R.; Johan, Z. Mineralogy of medieval slags from lead and silver smelting (Bohutín, Příbram district, Czech Republic): Towards estimation of historical smelting conditions. *Archeometry* **2009**, *51*, 987–1007. [[CrossRef](#)]
21. Kierczak, J.; Bril, H.; Neel, C.; Puziewicz, J. Pyrometallurgical slags in Upper and Lower Silesia (Poland): From environmental risks to use of slag-based products—A review. *Arch. Environ. Prot.* **2010**, *36*, 11–126.
22. Derkowska, K.; Świerk, M.; Nowak, K. Reconstruction of Copper Smelting Technology Based on 18–20th-Century Slag Remains from the Old Copper Basin, Poland. *Minerals* **2021**, *11*, 926. [[CrossRef](#)]
23. Sun, W.; Li, X.; Zhai, Q.; Li, J. Recovery of Valuable Metals from Nickel Smelting Slag Based on Reduction and Sulfurization Modification. *Minerals* **2021**, *11*, 1022. [[CrossRef](#)]
24. Viets, J.G.; Leach, D.L.; Lichte, F.E.; Hopkins, R.T.; Gent, C.A.; Powell, J.W. *Paragenetic and Minor-and Trace-Element Studies of Mississippi Valley-Type Ore Deposits of the Silesian-Cracow District*; Prace Państwowego Instytutu Geologicznego: Warsaw, Poland, 1996; Volume 154, pp. 51–71.
25. Popiołek, K. *Górnośląski Przemysł Górniczo-Hutniczy w Drugiej Połowie XIX Wieku*; Śląski Instytut Naukowy w Katowicach, PWN: Katowice, Poland, 1965; p. 245. (In Polish)
26. Hartshorne, R. The Upper Silesian Industrial District. *Geogr. Rev.* **1934**, *24*, 423–438. [[CrossRef](#)]
27. Górecki, W. *Rozwój Przemysłu na Górnym Śląsku w XVIII i XIX Wieku*; Silesia Progress: Luboszyce, Poland, 2018; p. 282. (In Polish)
28. Anyadike, N. *Lead and Zinc: Threats and Opportunities in the Years Ahead*; Woodhead Publishing Limited: Cambridge, UK, 2002; ISBN 1855735938.
29. Heijlen, W.; Muchez, P.H.; Banks, D.A.; Schneider, J.; Kucha, H.; Keppens, E. Carbonate-hosted Zn Pb deposits in Upper Silesia, Poland: Origin and evolution of mineralizing fluids and constraints on genetic models. *Econ. Geol.* **2003**, *98*, 911–932. [[CrossRef](#)]
30. Harańczyk, C. *Geochemia Kruszców Śląsko-Krakowskich złóż rud Cynku i Ołowiu*; Prace Geologiczne PAN: Kraków, Poland, 1965; Volume 5, pp. 1–111. (In Polish)
31. Górecka, E. *Mineral Sequence Development in the Zn–Pb Deposits of the Silesian-Cracow Area, Poland*; Polish Geological Institute: Warszawa, Poland, 1996; Volume 154, pp. 26–36.
32. Mayer, W.; Sass-Gustkiewicz, M. Geochemical characterization of sulphide minerals from the Olkusz lead-zinc ore cluster, Upper Silesia, (Poland), based on laser ablation data. *Mineral. Pol.* **1998**, *29*, 87–105.
33. Bauerek, A.; Cabala, J.; Smieja-Król, B. Mineralogical Alterations of Zn-Pb Flotation Wastes of the Mississippi Valley Type Ores (Southern Poland) and Their Impact on Contamination of Rain Water Runoff. *Pol. J. Environ. Stud.* **2009**, *18*, 781–788.
34. Jerzykowska, I.; Majzlan, J.; Michalik, M.; Göttlicher, J.; Steininger, R.; Błachowski, A.; Ruebenbauer, K. Mineralogy and speciation of Zn and As in Fe-oxide-clay aggregates in the mining waste at the MVT Zn–Pb deposits near Olkusz, Poland. *Geochemistry* **2014**, *74*, 393–406. [[CrossRef](#)]
35. Mikulski, S.Z.; Oszczepalski, S.; Sadłowska, K.; Chmielewski, A.; Małek, R. Trace Element Distributions in the Zn-Pb (Mississippi Valley-Type) and Cu-Ag (Kupferschiefer) Sediment-Hosted Deposits in Poland. *Minerals* **2020**, *10*, 75. [[CrossRef](#)]
36. Pierwoła, J.; Szuszkiewicz, M.; Cabala, J.; Jochymczyk, K.; Żogała, B.; Magiera, T. Integrated geophysical and geochemical methods applied for recognition of acid waste drainage (AWD) from Zn-Pb post-flotation tailing pile (Olkusz, southern Poland). *Environ. Sci. Pollut. Res.* **2020**, *27*, 16731–16744. [[CrossRef](#)]
37. Warchulski, R.; Mendecki, M.; Gawęda, A.; Sołtysiak, M.; Gadowski, M. Rainwater-induced migration of potentially toxic elements from a Zn–Pb slag dump in Ruda Śląska in light of mineralogical, geochemical and geophysical investigations. *Appl. Geochem.* **2019**, *10*, 104396. [[CrossRef](#)]
38. Violante, A.; Cozzolino, V.; Perelomov, L.; Caporale, A.G.; Pigna, M. Mobility and Bioavailability of Heavy Metals and Metalloids in Soil Environments. *J. Soil Sci. Plant Nutr.* **2010**, *10*, 268–292. [[CrossRef](#)]
39. Cabala, J.; Teper, L. Metalliferous Constituents of Rhizosphere Soils Contaminated by Zn–Pb Mining in Southern Poland. *Water Air Soil Pollut.* **2007**, *178*, 351–362. [[CrossRef](#)]

40. Cabala, J.; Krupa, P.; Misz-Kennan, M. Heavy Metals in Mycorrhizal Rhizospheres Contaminated By Zn–Pb Mining and Smelting Around Olkusz in Southern Poland. *Water Air Soil Pollut.* **2009**, *199*, 139–149. [[CrossRef](#)]
41. Cabala, J. Concentrations of Trace Elements in Zn–Pb Ores and Possibilities of Their Transfer to Waste Deposits. In *Conferencje Series; Research Reports of Central Mining Institute: Katowice, Poland, 1996; Volume 13*, pp. 17–32. (In Polish)
42. Coppola, V.; Boni, M.; Gilg, H.A.; Strzelska-Smakowska, B. Nonsulfide zinc deposits in the Silesia–Cracow district, Southern Poland. *Miner. Depos.* **2009**, *44*, 559–580. [[CrossRef](#)]
43. Sutley, S.; Sass-Gustkiewicz, M.; Mayer, W.; Leach, D. *Mineralogy and Chemistry of Oxidized Ores from the Upper Silesia Mississippi Valley-Type Zinc-Lead Deposits, Poland*; USGS Open File Report; USGS Publications Warehouse: Reston, VA, USA, 1999.
44. Keim, M.F.; Vaudrin, R.; Markl, G. Redistribution of silver during supergene oxidation of argentiferous galena: A case study from the Schwarzwald, SW Germany. *Neues Jahrb. Für Mineral.-Abh. J. Mineral. Geochim.* **2016**, *193*, 295–309. [[CrossRef](#)]
45. Bajda, T. Dissolution of mimetite $Pb_5(AsO_4)_3Cl$ in low-molecular-weight organic acids and EDTA. *Chemosphere* **2011**, *83*, 1493–1501. [[CrossRef](#)]
46. Kampf, A.; Mills, S.; Pinch, W. Plumboselite, $Pb_3O_2(SeO_3)$, a new oxidation-zone mineral from Tsumeb, Namibia. *Mineral. Petrol.* **2011**, *101*, 75–80. [[CrossRef](#)]
47. Lalinská-Voleková, B.; Majzlan, J.; Klimko, T.; Chovan, M.; Kučerová, G.; Michňová, J.; Hovorič, R.; Göttlicher, J.; Steininger, R. Mineralogy of weathering products of Fe–As–Sb mine wastes and soils at several Sb deposits in Slovakia. *Can. Mineral.* **2012**, *50*, 1207–1226. [[CrossRef](#)]
48. Bril, H.; Zainoun, K.; Puziewicz, J.; Courtin-Nomade, A.; Vanaecker, M.; Bollinger, J.-C. Secondary phases from the alteration of a pile of zinc-smelting slag as indicators of environmental conditions: An example from Świętochłowice, Upper Silesia, Poland. *Can. Mineral.* **2008**, *46*, 1235–1248. [[CrossRef](#)]
49. Turek, P.; Bajda, T.; Manecki, M. Dissolution of mimetite $Pb_5(AsO_4)_3Cl$ in malic acid solutions. *Mineral. Pol.* **2014**, *45*, 3–12. [[CrossRef](#)]
50. Clara, M.; Magalhaes, F. Arsenic. An environmental problem limited by solubility. *Pure Appl. Chem.* **2002**, *74*, 1843–1850. [[CrossRef](#)]
51. Twidwell, L.G.; Plessas, K.O.; Comba, P.G.; Dahnke, D.R. Removal of arsenic from wastewaters and stabilization of arsenic bearing waste solids—Summary Of Experimental Studies. *J. Hazard. Mater.* **1994**, *36*, 69–80. [[CrossRef](#)]
52. Kleszczewska-Zębala, A.; Manecki, M.; Bajda, T.; Rakovan, J.; Borkiewicz, O.J. Mimetite Formation from Goethite-Adsorbed Ions. *Microsc. Microanal.* **2016**, *22*, 698–705. [[CrossRef](#)] [[PubMed](#)]
53. Flis, J.; Manecki, M.; Bajda, T. Solubility of pyromorphite $Pb_5(PO_4)_3Cl$ –mimetite $Pb_5(AsO_4)_3Cl$ solid solution series. *Geochim. Cosmochim. Acta* **2011**, *75*, 1858–1868. [[CrossRef](#)]
54. Gołębiowska, B.; Pieczka, A.; Franus, W. Ca-bearing phosphatian mimetite from Rędziny, Lower Silesia, Poland. *Neues Jahrb. Für Mineral.* **2002**, *1*, 31–41. [[CrossRef](#)]
55. Kabata-Pendias, A. *Trace Elements in Soils and Plants*; CRC Press LLC: Boca Raton, FL, USA, 2001.
56. Migaszewski, Z.M.; Gałuszka, A. *Geochemia Środowiska*; PWN SA: Warsaw, Poland, 2016. (In Polish)
57. Neina, D. The Role of Soil pH in Plant Nutrition and Soil Remediation. *Appl. Environ. Soil Sci.* **2019**, *1*–9. [[CrossRef](#)]
58. McCauley, A.; Jones, C.; Olson-Rutz, K. *Soil pH and Organic Matter. Nutrient Management Module 8*; Montana State University: Bozeman, MT, USA, 2017.
59. Ochal, P.; Jadczyzyn, T.; Jurga, B.; Kopiński, J.; Matyka, M.; Madej, A.; Rutkowska, A.; Smreczak, B.; Łysiak, M. *Środowiskowe Aspekty Zakwaszenia Gleb w Polsce*; IUNG–PIB: Puławy, Poland, 2017. (In Polish)
60. Mayes, W.M.; Younger, P.L.; Aumônier, J. Hydrogeochemistry of Alkaline Steel Slag Leachates in the UK. *Water Air Soil Pollut.* **2008**, *195*, 35–50. [[CrossRef](#)]
61. Pandey, V.C.; Singh, N. Impact of fly ash incorporation in soil systems. *Agric. Ecosyst. Environ.* **2010**, *136*, 16–27. [[CrossRef](#)]
62. Caporale, A.G.; Violante, A. Chemical Processes Affecting the Mobility of Heavy Metals and Metalloids in Soil Environments. *Curr. Pollut. Rep.* **2015**, *2*, 15–27. [[CrossRef](#)]
63. López-Pamo, E.; Baretino, D.; Antón-Pacheco, C.; Ortiz, G.; Arránz, J.C.; Gumiel, J.C.; Martínez-Pledel, B.; Aparicio, M.; Montouto, O. The extent of the Aznalcóllar pyritic sludge spill and its effects on soils. *Sci. Total Environ.* **1999**, *242*, 57–88. [[CrossRef](#)]
64. Nieva, N.E.; Borgnino, L.; García, M.G. Long term metal release and acid generation in abandoned mine wastes containing metal-sulphides. *Environ. Pollut.* **2018**, *242*, 264–276. [[CrossRef](#)]

Disclaimer/Publisher’s Note: The statements, opinions and data contained in all publications are solely those of the individual author(s) and contributor(s) and not of MDPI and/or the editor(s). MDPI and/or the editor(s) disclaim responsibility for any injury to people or property resulting from any ideas, methods, instructions or products referred to in the content.